Heightened Cold-Denaturation of Proteins at the Ice-Water Inferface

Andrea Arsiccio,[†] James McCarty,[‡] Roberto Pisano,[†] and Joan-Emma Shea[*,¶,§]

[†]*Department of Applied Science and Technology, Politecnico di Torino, 24 corso Duca degli Abruzzi, Torino 10129, Italy*

[‡]*Department of Chemistry, Western Washington University, Bellingham, Washington 98225, United States*

[¶]*Department of Chemistry and Biochemistry, University of California, Santa Barbara, California 93106, United States*

[§]*Department of Physics, University of California, Santa Barbara, California 93106, United States*

E-mail: shea@ucsb.edu

Abstract

The process of freezing proteins is widely used in applications ranging from processing and storage of biopharmaceuticals to Cryo-EM analysis of protein complexes. The formation of an ice-water interface is a critical destabilization factor for the protein, which can be offset by the use of cryo-protectants. Using molecular dynamics simulation, we demonstrate that the presence of the ice-water interface leads to a lowering of the free-energy barrier for unfolding, resulting in rapid unfolding of the protein. The unfolding process does not require direct adsorption of the protein to the surface, but is rather mediated by nearby liquid molecules that show an increased tendency for hydrating non-polar groups. The observed enhancement in the cold denaturation

process upon ice formation can be mitigated by addition of glucose, that acts as a cryoprotectant through preferential exclusion from side-chains of the protein.

Introduction

Proteins generally function optimally at physiological temperature; however, practical considerations may make it necessary to place a protein under freezing conditions. For example, freezing is commonly used in the manufacturing process of biopharmaceuticals,[1] with water removed from the drug through lyophilization. Freezing is also used for long-term protein storage, as well as in cryo-EM studies and in spectroscopic studies such as DEER.[2–4] Freezing can however have detrimental effects on the protein, including denaturation, aggregation, and loss of biological activity. The conformational changes that may occur during freezing are linked to cold denaturation,[5–7] cryo-concentration, and formation of the ice-water interface.

Proteins experience reduced stability at extreme values of temperature; however, the effects of high and low temperature on protein conformations are remarkably different. Heat denaturation is entropically driven, as it is mainly dictated by the increase in conformational entropy associated with protein unfolding. In contrast, cold denaturation is enthalpically driven.[5,6,8–12] More specifically, at low temperature, the repulsive interaction between nonpolar residues and water is weaker, leading to a partial unfolding of the protein.[13–15] Water is a key player in cold denaturation,[9] and computational models employing an explicit description of the solvent have been applied to the study of this process.[16–18] For instance, it was found that cold unfolding can be driven by the increased stability of hydrogen bonds at the protein-water interface at low temperature, with shell water molecules forming hydrogen bonds more favorably than bulk water,[18] resulting in an overall enthalpic gain. Low-temperature unfolding occurs with an associated release of heat from the hydration shell, whereas the opposite is true in the case of heat-induced denaturation.[12]

The sharp reduction in temperature is not the only phenomenon that may be harmful to

protein stability during freezing.

~~and the cryo-concentration process also plays a central role. Physical properties related to concentration, such as ionic strength and relative composition of solutes, may change. For instance, freeze-concentration induced pH changes, due to selective crystallization of buffer components, may result in protein unfolding. This is particularly true when sodium or potassium phosphate buffers are used. Additionally, freezing polymer solutions may cause phase separation due to a change in polymer solubilities at low temperature. Phase separation creates a large interface that can promote protein denaturation. Furthermore, the protein will have a thermodynamic preference for one phase over the other and may partition into a phase with a low concentration of stabilizers. Finally,~~

The ice/freeze-concentrate interface, for instance, may loosen the native structure, leading to partial unfolding.[19–22] A clear experimental piece of evidence of ice formation-induced denaturation is the direct correlation between cooling rate and loss of biological activity, with more damage found at higher cooling rates.[23] This occurs because more rapid cooling results in smaller ice crystals, which expose a greater surface area to volume ratio than larger ones. In line with these considerations, solutions of the azurin protein exhibited a dramatic decrease in the average phosphorescence lifetime of the Trp-48 residue at the onset of ice formation, which is indicative of protein unfolding.[19]

Several phenomena can therefore adversely affect protein stability during freezing, but it has been shown that ice formation represents the most critical destabilizing factor.[24] For instance, using LDH as a model protein, a remarkable loss of activity was observed in frozen systems, while no degradation was detected in concentrated solutions at the same temperature and composition, but without ice. Hence, prevention of ice-induced denaturation is a key consideration whenever a protein is subjected to a freezing process.

The mechanism of ice-induced denaturation of proteins is difficult to pin down because of the lack of appropriate experimental techniques to address this problem. Strambini and Gabellieri[19] used intrinsic phosphorescence emission to demonstrate that the formation of ice

alters the native fold of proteins, and suggested that this perturbation may originate from the direct interaction between the protein and the ice surface. They also found that the addition of cryoprotectants such as glycerol and sucrose dramatically attenuates, or even eliminates, the loss of structure during freezing. It was therefore hypothesized that the stabilizing action of cosolutes should be regarded as a combined effect of lowering the freezing temperature and decreasing the adsorption affinity of the protein by coating the surface of ice. It has also been suggested[19] that the preferential exclusion of the cosolutes from the protein, which is believed to stabilize the native fold of proteins in the bulk,[25] may also contribute to an increased protein stability at the ice-water interface. However, the protective effect of these osmolytes against ice-induced denaturation is at present poorly understood.

The present work aims to provide insight into the effect of the ice-water surface on protein stability, and to clarify the role of cryoprotectants. For this purpose, all-atom Molecular Dynamics (MD) simulations are used. To overcome the timescale limitations of conventional MD, we employ the metadynamics enhanced sampling method[26] in its parallel bias variant.[27] Parallel bias metadynamics (PBMetaD) allows for a more complete sampling of the configurational state space without the limit of requiring only a very few number of collective variables. We also use the recent frequency adaptive metadynamics (FaMetaD)[28] method to obtain a rough estimate of kinetic properties. As a model protein for this investigation, we consider the 62 residue IgG-binding domain of peptostreptococcal protein L, which has been widely studied both experimentally[29–34] and computationally.[35,36] Protein L (see Figure 1) has a native fold with both an α-helix (res. ^{23}EKATSEAYAYADTL^{36}) and a β-sheet structure (res. ^{2}IKANLI^{7}, ^{13}TQTAEF^{18}, ^{43}WTV^{45} and ^{53}TLNIKF^{58}), which may be disrupted upon interaction with the ice-water surface. The stabilizing mechanism of common cryoprotectants is then investigated, with the aim to understand their effect at the ice-water interface. Glucose is considered as a model osmolyte, and its behavior at the ice surface is compared to its protective action in the bulk.

As previously mentioned, the ice surface was experimentally observed to promote un-

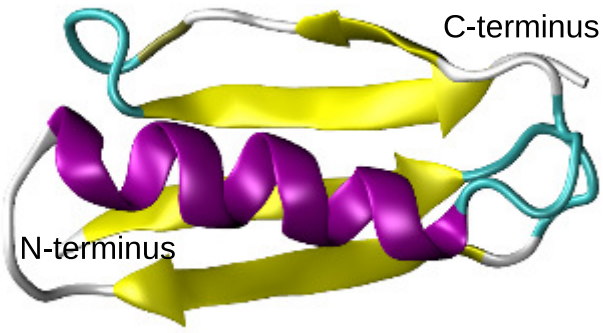

Figure 1: Cartoon structure of the IgG-binding domain of peptostreptococcal protein L, where the different secondary structure elements have been highlighted using different colors. purple: α-helix, yellow: extended β-sheet, cyan: turn, white: coil.

folding.[19–24] In line with this, we observe in our simulations that the unfolding process is characterized by a small free energy barrier in the presence of ice, and proceeds with faster kinetics than in bulk. However, experimental approaches have thus far not uncovered the mechanisms that lead to ice-induced unfolding. In this work, we put forth a possible explanation for these phenomena based on our atomistic-level simulations. More specifically, we suggest that the observed destabilization of the protein structure at the ice surface is due to an enhancement of cold denaturation phenomena, and is not mediated by direct adsorption. The addition of glucose is shown to stabilize the protein structure, because of preferential exclusion from specific patches on the protein surface.

Materials and Methods

Simulation details

All simulations were performed using Gromacs 5.1.4[37] patched with Plumed 2.4.1.[38] The protein L topology file was obtained from the RCSB Protein Data Bank (PDB: 2PTL[39]), and modified using the software Pymol to obtain the Y43W point mutant already studied in previous experimental works.[29,30] It was demonstrated that the Y43W mutation does not

cause significant perturbations of the wild type structure,[29] and was here introduced only to allow a direct comparison with experimental data. The OPLS-AA force field[40] was used, in combination with the TIP3P water model.[41] For simulations of glucose, the OPLS-AA-SEI force field[42] was employed.

The GenIce algorithm[43] was used to obtain an initial configuration of hexagonal (Ih) ice with proton disorder and zero dipole moment, and the generated ice layer (8.6 x 8.1 x 2.7 nm) was oriented with the basal {0001} plane in the direction of the liquid phase (z-axis). Afterwards, the Ih ice water molecules were kept frozen in place during the simulations.

Periodic boundary conditions were used, and the cut-off radius for both Coulombic (calculated using the PME method[44]) and Lennard-Jones interactions was 1.0 nm. 1 native protein molecule was introduced into each simulation box, and its charge was neutralized using Na^+ ions. After energy minimization with the steepest descent algorithm, the system was equilibrated for 5 ns at 1 bar and 260 K in the NPT ensemble, using Berendsen pressure and temperature coupling.[45]

The conformational stability of the IgG-binding domain of peptostreptococcal protein L was investigated both in bulk and at the ice-water interface, using parallel bias metadynamics (PBMetaD).[27] The effect of glucose on protein stability was also addressed. The PBMetaD simulations were then performed at 260 or 200 K and 1 bar in the NPT ensemble, controlling temperature and pressure with the V-rescale thermostat[46] and Parrinello-Rahman barostat,[47] respectively. Each simulation was run for a total time of 1.0 μs, using a 2 fs time step.

Parallel bias metadynamics

In parallel bias metadynamics,[27] multiple one-dimensional bias potentials, each acting on its own individual collective variable (CV), are simultaneously applied. As a result, a large number of CVs can be biased at a reasonable computational cost. This is useful in enhancing the exploration of phase space for systems with many degrees of freedom such as in the

case of protein conformational changes. We used a combination of the distance d between the protein center of mass (COM) and the ice-water interface, the protein α-helix (α), the protein antiparallel β-sheet (β) content, and the root mean square deviation (dRMSD) of the backbone atoms with respect to the reference structure as CVs. Details on the definition of these CVs and the metadynamics parameters are presented in the Supporting Information.

Table 1 summarizes the simulations performed. In simulations 1, 2 and 7 the bulk behavior of protein L was investigated, while simulations 3, 4 and 8 were aimed at studying the effect of the ice-water interface. In simulations 2 and 4, the number of glucose molecules within the box was adjusted so as to give a 1 M concentration. While in simulations 1-6 the simulated temperature (260 K) was above the onset of cold denaturation for protein L, the temperature used in simulations 7 and 8 (200 K) was selected to be low enough to result in cold unfolding. Converged free energy surfaces were computed using the reweighting technique of Tiwary et al.[48] Convergence of the free energy surface was assessed by monitoring the fluctuation of the one-dimensional free energy profiles obtained for the different CVs during the last 10% of the simulation time (see the Supporting Information, Figures S1-S6).

As a control, two unbiased simulations were performed in water and at the ice-water interface at 260 K, in absence of glucose (sim. 5 and 6 in Table 1).

Table 1: Details of the PBMetaD simulations performed*.

Sim. #	Surface	# Glucose Mol.	# Liquid Water Mol.	CVs	Box Dim. nm	T K
1	bulk	-	16733	α, β, dRMSD	8.0 x 8.0 x 8.0	260
2	bulk	308	14017	α, β, dRMSD	8.0 x 8.0 x 8.0	260
3	ice	-	18165	d, α, β, dRMSD	8.6 x 8.1 x 11	260
4	ice	335	15254	d, α, β, dRMSD	8.6 x 8.1 x 11	260
5	bulk	-	16733	unbiased	8.0 x 8.0 x 8.0	260
6	ice	-	18165	unbiased	8.6 x 8.1 x 11	260
7	bulk	-	16733	α, β, dRMSD	8.0 x 8.0 x 8.0	200
8	ice	-	18165	d, α, β, dRMSD	8.6 x 8.1 x 11	200

*1.0 μs simulation time for sim. 1-4 and 7-8, 100 ns simulation time for sim. 5-6

Kinetic analysis of the unfolding process

~~Recently, well-tempered metadynamics with an infrequent bias deposition rate was shown to give reliable residence time prediction of ligand-protein interactions, where the reaction coordinate was estimated using the spectral gap optimization of order parameters (SGOOP) method of Tiwary and Berne. Another study used a path CV to estimate the reaction coordinate of conformational transitions in T4 lysozyme mutants, obtaining rates again using metadynamics with an infrequent hill deposition rate.These methods are based on the hyperdynamics formalism , which requires a boost potential that strictly vanishes at the transitions state to ensure unbiased, ergodic sampling of the transition state region. Additionally, when the bias potential acts on a few low-dimensional order parameters as in metadynamics, the collective variables must be a good approximation of the reaction coordinate so that hidden slow degrees of freedom do not lead to orthogonal barriers which give rise to spurious rate predictions.~~

Frequency adaptive metadynamics (FaMetaD) was used to find approximate unfolding rates of protein L at 260 K, both in the bulk and at the ice-water interface. FaMetaD[28] is a variant of the metadynamics enhanced sampling method where the bias deposition frequency is adjusted during the simulation time. The bias deposition frequency is quick at the beginning of the simulation, to quickly fill up the free energy basins, but is then reduced as the system moves close to the transition state region, in order to minimize the risk of biasing the free energy barriers. Low dimensional approximate representations of the reaction coordinate were used for this investigation. Computational details about the definition of these reaction coordinates and the kinetic analysis can be found in the Supporting Information.

Results and Discussion

Protein L is destabilized by the presence of ice, while glucose has a cryoprotective effect both in the bulk and at the ice surface

Using PBMetaD simulations, we computed the free energy surfaces (FES) for protein L, both in the bulk and in the presence of the ice-water interface. The presence of glucose as a model cryoprotectant was also considered. The results obtained at 260 K are shown in Figure 2, where the FES as a function of the antiparallel β-sheet content (β) and radius of gyration R_g or the α-helix content (α) and dRMSD are shown in the left and middle panel, respectively. The three most sampled conformations were identified in each FES, and labeled with a letter followed by a number. The letter N corresponds to the most folded (native-like) structure, while letters A and B were used to identify two partially folded conformations, where either the α-helix content (conformation A) or the antiparallel β-sheet content (conformation B) have been lost to some extent. The number in each label is then used to distinguish between the different simulations, as listed in the first column of Table 1.

The relative contribution in the FES as a percentage of each of these conformations was also computed as,

$$P_X = \frac{\int_X ds e^{-\beta F(s)}}{\int ds e^{-\beta F(s)}} \tag{1}$$

where $F(s)$ is the free energy, and the integral in the numerator is over a subset of the volume that defines basin X = N, A or B. The calculated percentages are also displayed under the cartoon of each structure in the right panel of Figure 2.

260 K is still above the onset of cold denaturation for protein L. As a result, the native fold remained the most probable (>98%) in bulk water (Figure 2a), even though both the β-sheet and α-helix content could be partially lost upon unfolding. For instance, structure A1 ($\approx$ 1.63% probability) showed values of α-helix content α as low as 2, and conformation

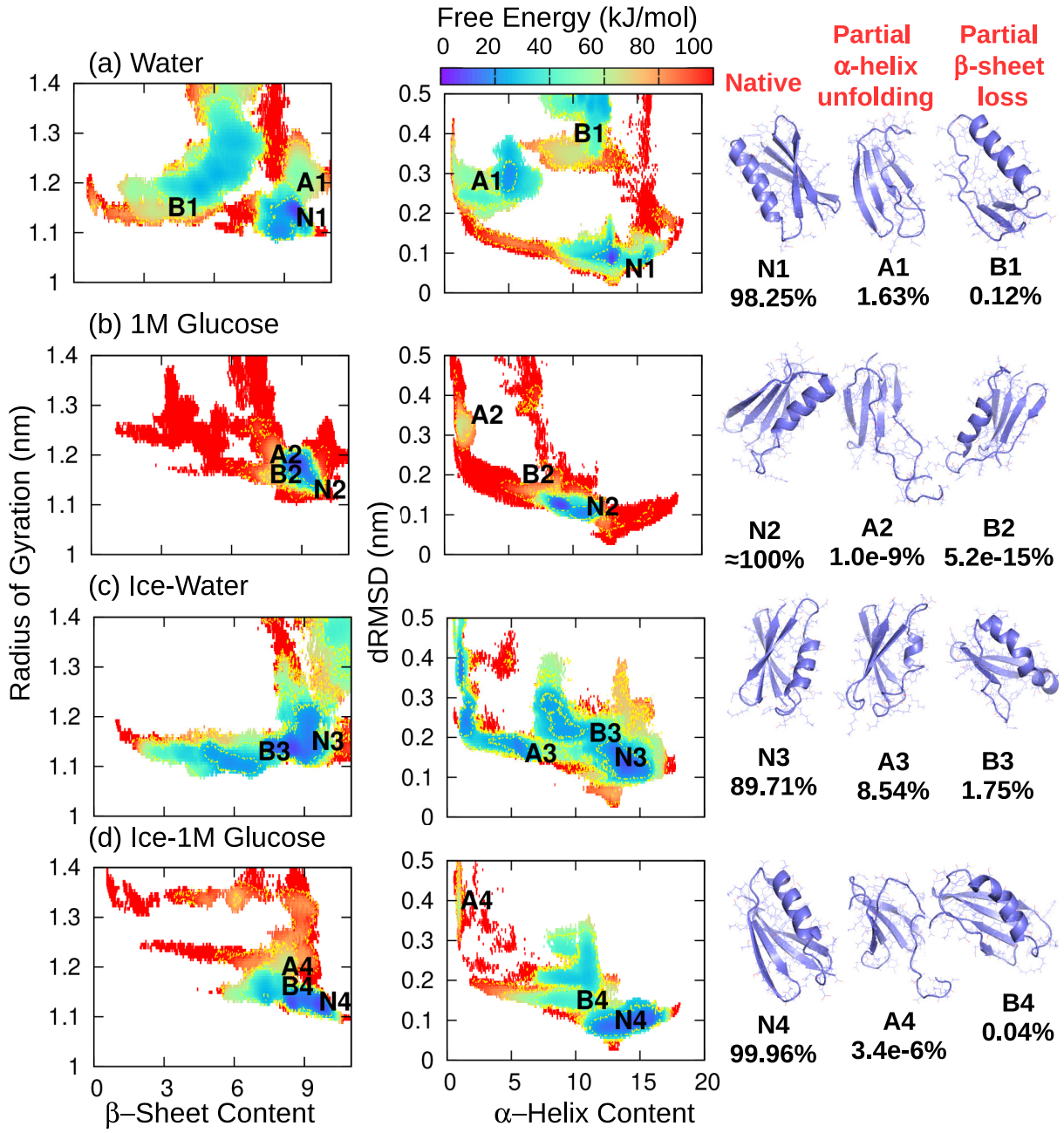

Figure 2: Free energy surface (FES) as a function of β-sheet content and radius of gyration (left) or α-helix content and dRMSD (center) for (a) bulk-water (sim. 1), (b) 1M glucose (sim. 2), (c) ice-water interface (sim. 3) and (d) ice-1M glucose interface (sim. 4). The letters on the FES identify the most sampled protein conformations. A cartoon of each structure, with the relative contribution as a percentage of these conformations, is also shown on each line in the right-hand panel. N refers to the native structure, A refers to structures with partial α-helix loss, and B refers to structures with partial β-sheet loss.

B1 ($\approx 0.12\%$ probability) was characterized by β-sheet content $\beta = 4$, compared to values of 15 and 9.5 for α and β, respectively, in structure N1 (Figure 2a).

Upon addition of glucose (Figure 2b), the FES was restricted toward more folded conformations (the relative contribution of unfolded conformations was on the order of $1.0 \cdot 10^{-9}\%$ or $5.2 \cdot 10^{-15}\%$ for A2 and B2, respectively). In this case, the β-sheet structure was remarkably stabilized, with conformation B2 still showing a significant β-sheet content ($\beta = 7.6$). An almost complete loss of the α-helix content was still possible ($\alpha = 2$ for structure A2), but the free energy barrier for this unfolding process was significantly higher than in bulk water. The stabilizing effect of glucose observed in our simulations is in line with the experimental results of Plaxco and Baker,[31] where the addition of 1M glucose was found to produce a 1 kcal/mol increase in the free energy of unfolding for protein L.

In contrast, the free energy barrier of unfolding was reduced by the presence of the ice-water interface, as shown in Figure 2c. The folded conformation N3 could in fact lose its β-sheet ($\beta \approx 6$ or lower in structure B3, having probability 1.75 %) or α-helix content ($\alpha < 5$ in structure A3, having probability 8.54 %) almost without free energy penalty.

Finally, Figure 2d shows that glucose has a stabilizing effect also at the ice-water surface, again restricting the FES toward more folded conformations and significantly hindering the loss of β-sheet content ($\beta \approx 7$ in structure B4, characterized by 0.04 % probability). The loss of α-helix content is still possible in the presence of glucose (α=1 in structure A4, that shows a low probability, on the order of $10^{-6}\%$), but a quite large energy barrier characterizes this unfolding process.

A lower temperature (200 K) at which cold unfolding should be more pronounced was also considered (sim. 7-8 in Table 1), and the results obtained in these conditions are shown in Figure 3.

In this case, the native fold was extremely unstable ($< 0.1\%$) both in bulk water and at the ice-water interface. Because of this, it was difficult to distinguish any remarkable worsening of protein stability in presence of the ice surface. At this lower temperature, the protein

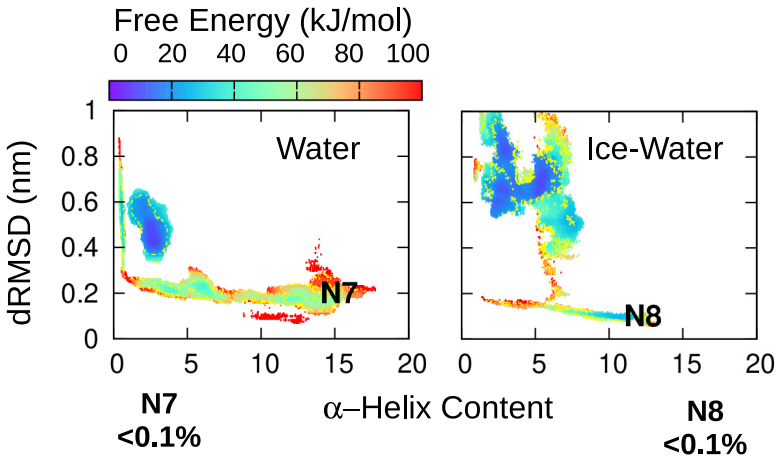

Figure 3: Free energy surface (FES) as a function of α-helix content and dRMSD for bulk-water (sim. 7, left), and the ice-water interface (sim. 8, right) at 200 K. The letters on the FES identify the native conformation, which in this case is extremely unstable. The relative contribution of the native structure to the FES was found to be lower than 0.1 %, as shown under the graphs.

could explore a wide ensemble of unfolded structures, and the identification of representative configurations for the denatured state was complicated by this extreme instability. For this reason, we will focus our next investigation on the simulations performed at 260 K, where a difference in protein behavior at the ice surface, compared to the bulk, can clearly be identified. Moreover, this also represents a realistic case study, as the denaturing effect of the ice surface has been experimentally observed to occur immediately after the formation of ice, and in temperature ranges where the protein is still stable in bulk.[19]

It is interesting and important to note that a completely unfolded structure was never sampled in our simulations. Each protein conformation still preserved some secondary structure, either α-helix or β-sheet, and a large increase in the radius of gyration was never observed. For instance, the folded structure was characterized by $R_g \approx 1.1$ nm, and values of R_g larger than 1.5 nm were rarely sampled. This observation that the protein does not unfold completely can be explained considering that our simulations were performed at low temperature (260 or 200 K) with a relatively low metadynamics bias factor relative to the energy barrier associated with unfolding. Under these conditions, cold denaturation typi-

cally ensues. While heat denaturation is favored by the increase in conformational entropy as the protein unfolds to a largely extended conformation, cold denaturation is enthalpically driven. As a result, cold-denatured proteins are more compact, partially unfolded conformations, showing a mild form of structural loss.[12–15] It is interesting to note that the presence of the ice-water interface does not alter the typical features of cold denaturation, leading to the formation of compact, partially folded conformations.

The protein segments which were mostly involved in the unfolding process were also investigated. In order to do this, the backbone RMSD of the protein conformations sampled during the simulations was computed, using N1 as reference structure (see Figure S7). As previously mentioned, we focused our attention on the simulations performed at 260 K, as in these conditions it is easier to identify representative unfolded configurations, and the effect of the ice surface can more clearly be distinguished. This analysis showed that residues ^{13}TQTAEFKGTFEKATSEAY^{30} generally were the most prone to undergo the unfolding process. This segment includes one β-strand (residues ^{13}TQTAEF^{18}), and a large part of the α-helix (residues ^{23}EKATSEAY^{30}). However, in the presence of ice (conformation B3), the amino acid sequence ^{2}IKANLIFANGSTQTA^{16} was also significantly involved in the loss of secondary structure. Therefore, in this case the β-strand ^{2}IKANLI^{7} was also disrupted. Finally, residues ^{33}ADTLKKDNGEWT^{44} showed a larger RMSD when glucose was added to the simulation box. This was true not only for the unfolded conformations B2 and B4, but also for the folded structures N2 and N4. This may indicate that the presence of glucose promotes the sampling of protein structures where this amino acid sequence is more expanded than in pure water. To further confirm this observation, structures N1, N2 and N4 were aligned using the STAMP (Structural Alignment of Multiple Proteins) program.[49] STAMP aligns protein structures by applying optimal rigid-body rotations and translations in order to minimize the C_α distance between corresponding residues of each conformation. In Figure 4a the three superimposed structures are identified by different colors, and residues 33-44 are highlighted in yellow. In Figure 4b the same aligned structures are shown, but the coloring

method allows identification of the zones (displayed in red) where the conformations are structurally different. Comparison of Figures 4a and 4b confirms that residues 33-44 are the most involved in expansion in presence of glucose, even though the structural modification is not dramatic.

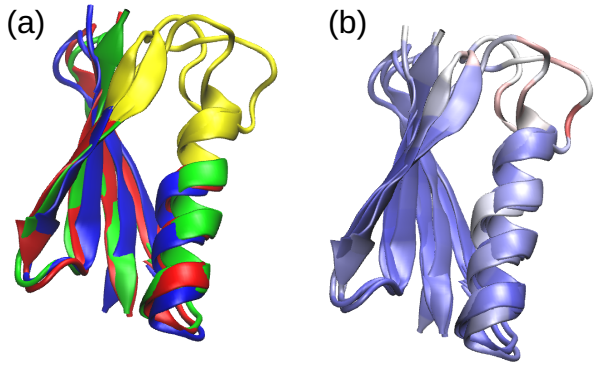

Figure 4: (a) N1 (red), N2 (blue) and N4 (green) structures after alignment with the STAMP program.[49] Residues 33-44 have been highlighted in yellow. In (b), the same image is shown, but a different coloring is used, where the blue areas correspond to structurally similar zones, and the red color indicates poor alignment.

The ice surface promotes loss of protein structure by enhancing cold denaturation phenomena

Having established that the ice surface has a destabilizing effect on the protein structure by lowering the free energy barrier for the unfolding process, we turn to an analysis of the interaction of protein L with the ice surface. Remarkably, our analysis revealed that no direct interaction occurred between protein L and the ice-water surface. For instance, Figure 5a shows that the minimum distance between the protein and the ice interface generally remained quite large, both at 260 and 200 K. This was true for both the whole protein (black bars), and those amino acid sequences which were the most prone to unfold according to our RMSD analysis (residues 13-30 in red, and residues 2-16 in green). The number of protein-ice hydrogen bonds (Figure 5b) remained low during the simulations as well, with an average value of 0.0708 at 260 K and $4.22 \cdot 10^{-6}$ at 200 K. This means that the

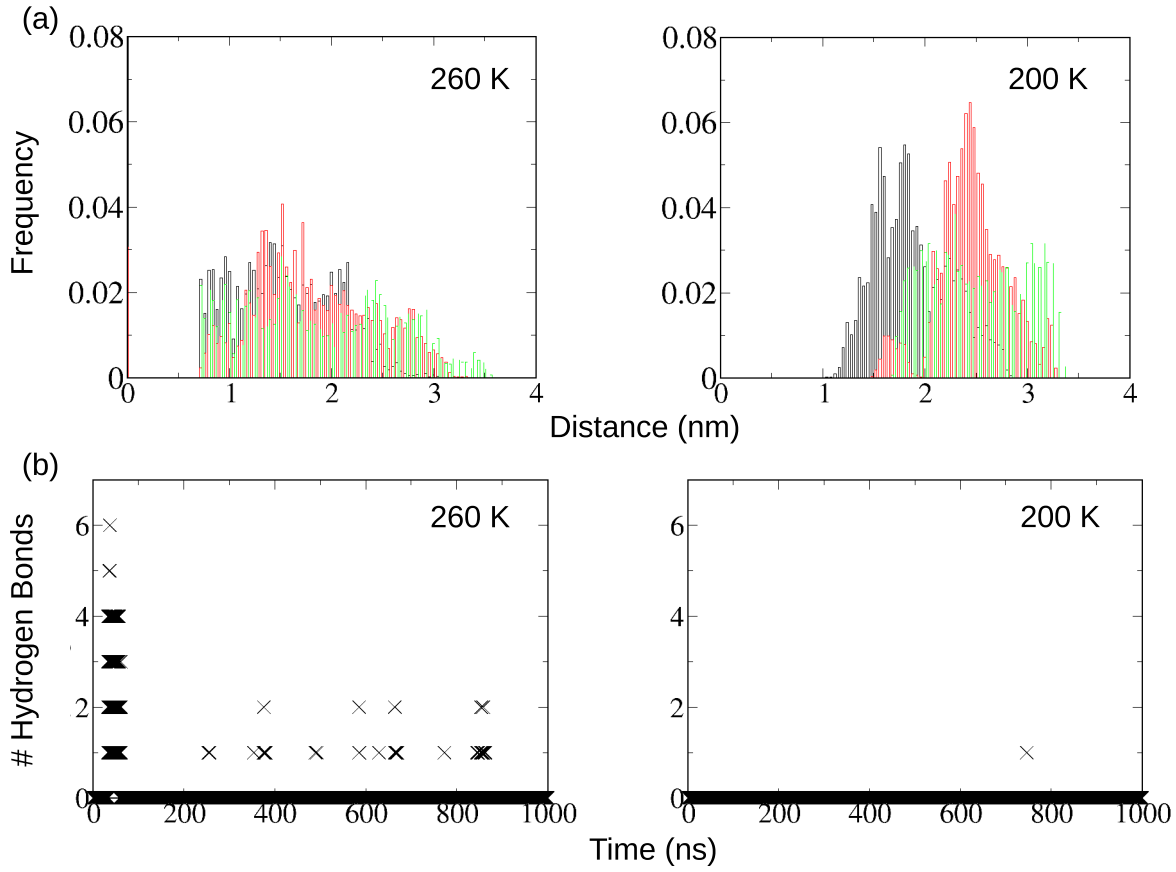

Figure 5: (a) Histogram showing the distribution of the minimum distance between the ice-water interface and the whole protein (black bars), residues 13-30 (red bars) and residues 2-16 (green bars). (b) Number of proten-ice hydrogen bonds as function of the simulation time. The results refer to simulations 3 and 8 in Table 1.

direct interaction between the protein and the ice surface cannot account for the observed destabilization of the protein structure, consistent with earlier work on the GB1 protein.[50] In addition, solid-state NMR studies suggest that the hydration shell of soluble proteins does not freeze below the freezing temperature of the bulk solution.[51,52] Siemer et al.[53] observed that ubiquitin at -35 °C keeps its entire hydration shell, which prevents interaction with the ice lattice. The authors further suggest that most soluble proteins are likely to behave like ubiquitin, and that their hydration shell does not freeze until a temperature which is much lower than the equilibrium freezing value.[54] Above this temperature, according to NMR measurements, no direct interaction is possible between the protein and the ice surface. More recently,[55] X-ray diffraction studies of protein/ice interaction further suggested that two common pharmaceutical proteins, recombinant human albumin and a monoclonal antibody, interacted with ice crystals indirectly, by accumulating in the liquid-like layer above the ice surface, rather than by direct adsorption. Smaller protein molecules, such as lysozyme, were found to partition even further from the ice interface, in line with our simulations. We note that a different behavior from the one observed here can be found for a specialized class of proteins, antifreeze proteins (AFPs), that can directly bind to ice nuclei and prevent them from growing.[55–57]

~~For instance, inhibition of growth of both basal and prism planes by AFPs has been observed. It was first suggested that the hydrophilic groups on the ice-binding sites of AFPs could hydrogen-bond with ice, favoring direct adsorption. However, it was later discovered that hydrophobic residues are largely present on the ice-binding sites of AFPs, indicating that hydrophilic interaction cannot be the only explanation. Simulation results suggested that the peculiar behavior of AFPs may be related to the arrangement of water molecules in proximity of the ice-binding sites, where a slight increase in tetrahedral order and slower relaxation dynamics are observed. Another study suggested that both hydrophobic and hydrophilic groups are involved in ice-binding, and that water molecules adopt a highly ordered structure, forming a clathrate-like shell around the ice-binding site of AFPs. These ordered~~

~~water molecules may be released when binding to ice, resulting in overall gain of entropy. However, molecular simulations indicate that the ordered structure of water molecules at the ice-binding site is only formed after the AFP has moved next to the ice surface, meaning that a preordering of hydration water is not necessary for ice recognition. NMR studies on frozen solutions further suggest that only the portion of AFPs hydration shell at the ice-binding site is in contact with the ice lattice. The remaining part of the hydration shell behaves similarly to the hydration shell of non-ice-interacting proteins, and hence does not freeze. Overall, this suggests that the ice surface may lead to remarkable modifications in the hydration water of AFPs, and the exixtence of a similar effect on protein L was investigated in our simulations.~~

We also calculated the diffusion coefficient of the liquid water molecules in (unbiased) simulations 5 and 6, by least squares fitting a straight line through the mean square displacement as function of time. According to the Einstein relation, the slope of this line should be directly related to the diffusion coefficient. We found that the diffusion coefficient was $2.9138 \pm 0.0123 \cdot 10^{-5}$ cm^2/s in absence of ice (simulation 5), while it decreased to $1.8733 \pm 0.0084 \cdot 10^{-5}$ cm^2/s when an ice layer was added to the simulation box (simulation 6). Therefore, the presence of the ice surface slows down the nearby layers of liquid water molecules. We further verified whether this also translated into increased ordering of the water molecules. The tetrahedral order parameters S_g and S_k [58] were computed for simulations 5 and 6, as detailed in the Supporting Information. For a perfect tetrahedron, S_g and S_k equal 0, while their value increases as the configuration deviates from tetrahedrality. In Figure S8 the average value of these order parameters as function of the z coordinate over the equilibrated trajectory (last 50 ns) is shown. In the case of simulation 5 (bulk water, red curve) both order parameters are significantly different from 0, indicating, as expected, absence of any ordering. For instance, S_g is close to 0.25, which is the expected value for randomly arranged bonds. In the case of simulation 6 (presence of an ice layer, black curve) both S_g and S_k are 0 in correspondence of the ice layer ($0 < z < 2.7$ nm), but their value in the liquid layers above the ice surface is similar to the case of bulk water (simulation 5),

indicating that these layers do not show any significant tetrahedral arrangement.

Additionally, we computed the average number of hydrogen bonds between the liquid water molecules and the whole protein, or those regions that were more prone to unfold (residues 2-30 according to our RMSD analysis). Simulations 1, 3, 7 and 8 in Table 1 revealed that, at equal temperature, both the whole protein (Figure 6a) and residues 2-30 (Figure 6b) formed more hydrogen bonds with liquid water at the ice surface (red and blue bars) than in bulk water (black and green bars). It is also interesting to note that the number of hydrogen bonds increased at lower temperature (200 K, green and blue bars). The increased protein hydration at the ice surface was confirmed also in the unbiased simulations 5 and 6. As illustrated in Figure 6c, we found that the degree of protein-solvent interaction increased in presence of ice, with the number of hydrogen bonds moving from 155 $\pm$ 6 (sim. 5) to 164 $\pm$ 7 (sim. 6) for the whole protein, from 51 $\pm$ 3 (sim. 5) to 57 $\pm$ 4 (sim. 6) for residues 13-30, and from 24 $\pm$ 2 (sim. 5) to 31 $\pm$ 3 (sim. 6) for residues 2-16. This last region of the protein includes the β-strand ^{2}IKANLI^{7}, and was significantly involved in the loss of secondary structure only in presence of ice. Correspondingly, we observed that the number of hydrogen bonds formed by these residues with liquid water not only increased upon ice formation, but these bonds were also significantly stronger. We computed the average hydrogen bonds lifetime,[59–61] that is a good indicator of the hydrogen bond strength. We observed that the liquid water molecules in simulation 6, slowed down by the presence of ice, could form hydrogen bonds with residues 2-16 that lasted, on average, 25 ps, i.e. around 13 times more than in pure water (about 1.9 ps in simulation 5).

This analysis suggests that the destabilizing effect of the ice interface should not be related to direct adsorption onto the surface, but should rather be mediated by a modification of the nearby liquid water behavior toward the protein. Within this framework, the effect of the ice surface could be explained as an enhancement of the cold denaturation phenomena. As previously mentioned, cold denaturation is the result of an increased tendency for nonpolar group hydration.[5,11] The free energy penalty for the interaction between water and the

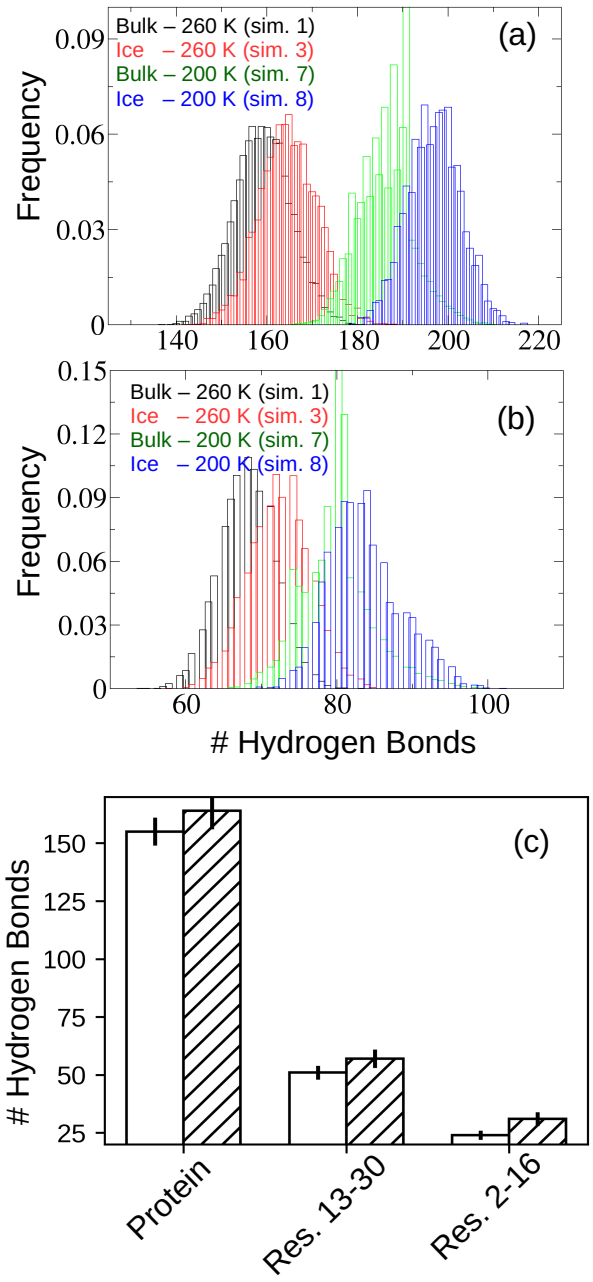

Figure 6: (a-b) Histogram showing the distribution of hydrogen bonds between liquid water molecules and (a) the whole protein or (b) residues 2-30. The black, red, green and blue bars correpond to simulations 1 (bulk water - 260 K), 3 (ice-water interface - 260 K), 7 (bulk water - 200 K), or 8 (ice-water interface - 200 K) in Table 1, respectively. (c) Bar graph showing the number of hydrogen bonds between liquid water molecules and the whole protein, residues 13-30 or residues 2-16 in the case of bulk water (plain bars) or at the ice-water interface (dashed bars). The results refer to simulations 5 and 6 in Table 1.

hydrophobic patches of the protein becomes smaller as the temperature is decreased, leading to the observed loss of structure. In line with this, we observed that the number of protein-water hydrogen bonds increased at lower temperature (200 K, green and blue bars in Figures 6a,b). Moreover, we also found that, in the presence of ice, the nearby liquid water molecules did not arrange in an ordered structure, but were anyway remarkably slowed down, and could therefore form a large number of strong hydrogen bonds with specific regions of the protein. These regions show a slightly larger nonpolar surface area (the ratio of the nonpolar to total surface area S_{np}/S is 0.53 and 0.52 for residues 13-30 and 2-16, respectively) if compared to the protein average ($S_{np}/S = 0.49$). As a result, these amino acid sequences, poorly hydrated in the folded structure, interact more favorably with water in the presence of ice (Figure 6), assuming an extended conformation. The ice surface therefore promotes the solvent penetration of poorly hydrated regions in the folded structure, which is a characteristic feature of the cold denaturation process.

~~The observed effect of the ice surface on the surrounding liquid water molecules, and on the protein structure, may also be at the basis of the ice-binding properties of AFPs. In this case, the observed slowdown of water molecules, and consequent solvent penetration of the protein structure, may induce the ordering of the water molecules at the ice-binding site. The hydration shell of AFPs, disordered in the bulk solution, could therefore transform into a clathrate-like structure close to the ice surface, and this may promote direct adsorption. A similar ordering process is not observed for other protein molecules (such as protein L herein investigated, see Figure S8), which accumulate further from the surface.~~

Glucose stabilizes the native structure by being preferentially excluded from specific regions of the protein

The mechanism of protein stabilization by glucose was further analyzed. According to the preferential exclusion mechanism,[25,62,63] the protective osmolytes should stabilize the native state by being preferentially excluded from the protein surface. A possible way to quantify

differences in the degree of preferential exclusion from specific patches on the protein surface is to compute the following relative distribution of glucose molecules,

$$\text{Relative distribution of glucose molecules} = \frac{(n_g(1\text{ nm})/n_{all}(1\text{ nm}))_1}{(n_g(1\text{ nm})/n_{all}(1\text{ nm}))_2} \quad (2)$$

where $n_g(1\text{ nm})$ and $n_{all}(1\text{ nm})$ are the coordination number of glucose and water + glucose molecules, respectively, at 1 nm from the surface of patch 1 (numerator) or 2 (denominator). A value of the relative distribution parameter larger than 1 indicates that glucose interacts more with region 1 than with region 2, and vice versa.

The relative distribution parameter of glucose molecules for residues 33-44 (patch 1) over residues 2-30 (patch 2) is shown in Figure 7a.

Figure 7a reveals that glucose interacted with different regions of the protein to a different extent. The relative distribution parameter showed an average value of 1.132, indicating that glucose was attracted by residues 33-44, while it interacted less favorably with residues 2-30. Interestingly, the protein region including amino acids 33-44 was more expanded upon addition of glucose than in bulk water, as evidenced by our RMSD and alignment analyses (Figures S7 and 4). In contrast, a 1M glucose concentration promoted a more collapsed conformation of residues 2-30, which were the most prone to undergo cold denaturation.

According to these results, we conclude that glucose stabilizes the native fold by being excluded from the hydrophobic, unfolding-prone regions of the protein. However, glucose promotes a slightly different native state, because of preferential interaction with residues 33-44. The glucose molecules may be particularly attracted by this amino acid sequence because of its hydrophilicity ($S_{np}/S = 0.43$ for residues 33-44, compared to an average value $S_{np}/S = 0.49$ for the protein and $S_{np}/S = 0.53$ for residues 2-30).

The observation that the preferential exclusion from specific amino acid sequences is key for protein structural preservation is in line with previous observations,[64] and suggests the interpretation of the preferential exclusion mechanism as a variant of the poor solvent theory for polymers. It is well known that the random coil of a polymer adopts an unfolded confor-

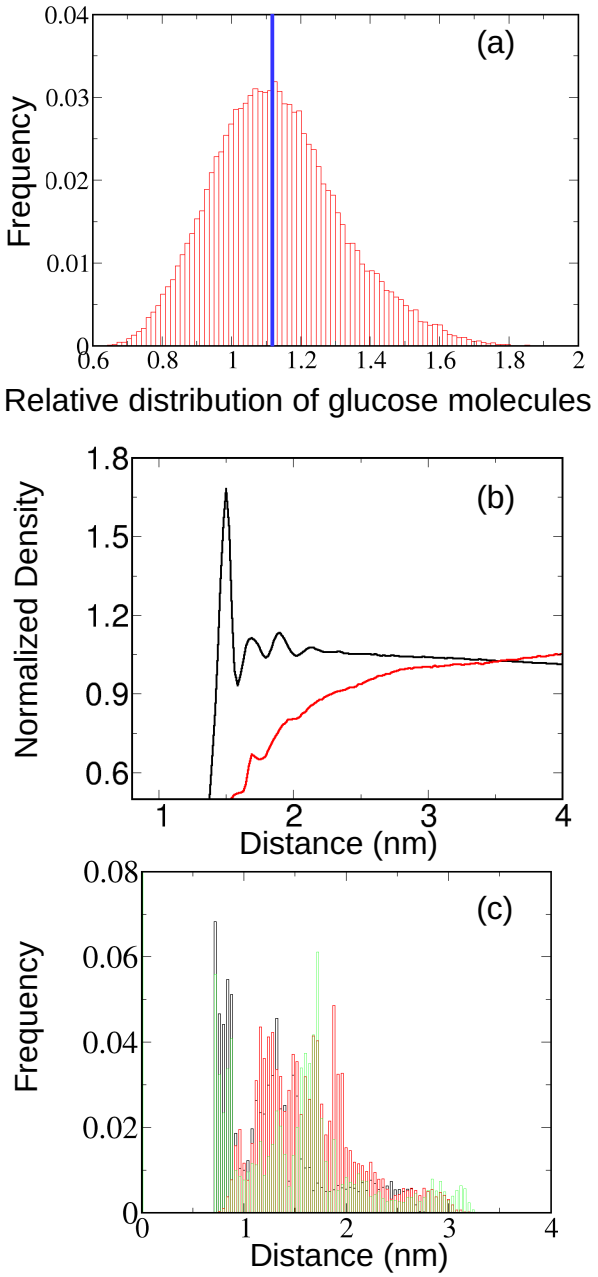

Figure 7: (a) Relative distribution parameter of glucose molecules for residues 33-44 (patch 1) over residues 2-30 (patch 2). The average of the distribution is displayed as a vertical blue line in the graph. (b) Density of water (black line) and glucose (red line) as function of the distance from the ice-water interface. The density was normalized to the bulk value. (c) Histogram showing the distribution of the minimum distance between the ice-water interface and the whole protein (black bars), residues 13-30 (red bars) and residues 2-16 (green bars). The results refer to simulation 4 in Table 1.

mation in a good solvent, while a more collapsed conformation is sampled in a poor solvent. Proteins represent a particularly heterogeneous class of polymers, and their surface often exposes patches with extremely different features, in terms of hydrophilicity/hydrophobicity or surface charge. As a result of this heterogeneity, it is not easy to define a poor solvent for a protein as a whole, and a good solvent for specific patches on the protein surface could be, at the same time, a poor solvent for other amino acid sequences of the same protein. In this framework, glucose proved to be a good solvent for residues 33-44 of protein L, but a poor solvent for the hydrophobic region formed by amino acids 2-30.

It has also been suggested[19] that polyols and sugars may stabilize the native fold by coating the surface of ice and decreasing the adsorption affinity of the protein. However, we did not observe a direct adsorption of protein L to the ice-water interface in our simulations (Figure 5). Moreover, Figure 7b indicates that glucose was not attracted to the ice surface, and could therefore not form a coating of adsorbed molecules at the ice-water interface. The stabilizing mechanism of glucose is therefore not related to a decreased protein adsorption, at least in the case of protein L. In contrast, the protein approached the ice-water interface similarly in 1M glucose (Figure 7c) and in pure water (Figure 5a).

Kinetic analysis

Using the frequency adaptive metadynamics approach, we can estimate the relative difference in unfolding times of the protein in the presence and absence of ice. The details of the calculations are shown in the SI. Although the unfolding times reported in the SI can only be taken as estimates, they nonetheless permit a discussion of general trends. According to our results, the unfolding process is faster at the ice surface than in bulk water even though the presence of ice slows down the motion of the surrounding water molecules. As shown in Figure 2, we observed that the ice surface promotes a significant reduction in the free energy of unfolding. The FaMetaD simulations further show that this lowering of the energy barrier translates into an extremely fast denaturation process. Hence, the process of ice formation

represents a critical destabilizing factor for protein stability, from both a thermodynamic and a kinetic point of view.

Conclusions

We have investigated the stability of protein L at the ice surface, and compared the results to the case of bulk water. We observed a significant reduction in the free energy of unfolding at the ice surface at 260 K, which translated into a fast denaturation process. This is in line with the decrease in protein stability that is experimentally observed.[19–24] However, augmenting experimental results, our simulations reveal a possible explanation to this observation. We observe that the ice interface modifies the properties of the nearby liquid water molecules, slowing down their motions and promoting the hydration of the nonpolar groups of the protein. The solvent penetration of nonpolar regions is a characteristic feature of cold denaturation, which seems to be dramatically enhanced in the presence of the ice-water interface. We also showed that glucose can counteract the ice-induced unfolding process, likely by being preferentially excluded from the hydrophobic patches of the protein rather than through decreased adsorption affinity of the protein in the presence of glucose. Our simulations shed new insights into the stabilizing action of common cryoprotectants at the ice-water interface, and suggest that consideration of specific interactions between ice and the protein should not be the main, or only, concern when designing a formulation to be frozen.

Acknowledgement

The authors acknowledge support from the hpc@polito team (http://www.hpc.polito.it), from the Center for Scientific Computing at the California Nanosystems Institute (CNSI), MRL: an NSF MRSEC (DMR-1720256) and NSF CNS-1725797, and we also acknowledge the CINECA award under the ISCRA initiative (ProtExc-HP10C1MQDX and Cys-Surf-

HP10CSOLZQ), for the availability of high performance computing resources and support. JES acknowledges support from the NSF (MCB-1716956) and the NIH (R01GM118560). We used the Extreme Science and Engineering Discovery Environment (XSEDE) Stampede2 at the Texas Advanced Computing Center (TACC) through allocation TG-MCA-05S027.

Supporting Information

Details on parallel bias metadynamics simulations, convergence of the simulations, RMSD analysis of protein regions involved in the unfolding process, tetrahedral order parameters for water molecules in presence and absence of the ice surface, kinetic investigation of protein L unfolding.

References

(1) Authelin, J.-R.; Rodrigues, M. A.; Tchessalov, S.; Singh, S.; McCoy, T.; Wang, S.; Shalaev, E. Freezing of biologicals revisited: Scale, stability, excipients, and degradation stresses. *J. Pharm. Sci.* **2020**, *109*, 44–61.

(2) Junpeng, D.; Davies, D. R.; Goragot, W.; Wu, M.; Hol, W. G. J.; Christopher, M. An Improved Protocol for Rapid Freezing of Protein Samples for Long-Term Storage. *Acta Cryst. D* **2004**, *60*, 203–204.

(3) Nitin, R.; Rajan, R. S. Current Perspectives on Stability of Protein Drug Products during Formulation, Fill and Finish Operations. *Biotechnol. Progress* **2008**, *24*, 504–514.

(4) Radmanovic, N.; Serno, T.; Joerg, S.; Germershaus, O. Understanding the Freezing of Biopharmaceuticals: First-Principle Modeling of the Process and Evaluation of Its Effect on Product Quality. *J. Pharm. Sci.* **2013**, *102*, 2495 – 2507.

(5) Privalov, P. L. Cold Denaturation of Proteins. *Crit. Rev. Biochem. Mol. Biol.* **1990**, *25*, 281–305.

(6) Franks, F. Protein Destabilization at Low Temperatures. *Adv. Protein Chem.* **1995**, *46*, 105–139.

(7) Yan, R.; DeLos Rios, P.; Pastore, A.; Temussi, P. A. The cold denaturation of IscU highlights structure–function dualism in marginally stable proteins. *Commun. Chem.* **2018**, *1*, 13.

(8) Dill, K. A.; Alonso, D. O. V.; Hutchinson, K. Thermal Stabilities of Globular Proteins. *Biochemistry* **1989**, *28*, 5439–5449.

(9) Graziano, G. On the mechanism of cold denaturation. *Phys. Chem. Chem. Phys.* **2014**, *16*, 21755–21767.

(10) Graziano, G.; Catanzano, F.; Riccio, A.; Barone, G. A Reassessment of the Molecular Origin of Cold Denaturation. *J. Biochem.* **1997**, *122*, 395–401.

(11) Lopez, C. F.; Darst, R. K.; Rossky, P. J. Mechanistic Elements of Protein Cold Denaturation. *J. Phys. Chem. B* **2008**, *112*, 5961–5967.

(12) Matysiak, S.; Debenedetti, P. G.; Rossky, P. J. Role of Hydrophobic Hydration in Protein Stability: A 3D Water-Explicit Protein Model Exhibiting Cold and Heat Denaturation. *J. Phys. Chem. B* **2012**, *116*, 8095–8104.

(13) Davidovic, M.; Mattea, C.; Qvist, J.; Halle, B. Protein Cold Denaturation as Seen From the Solvent. *J. Am. Chem. Soc.* **2009**, *131*, 1025–1036.

(14) Babu, C. R.; Hilser, V. J.; Wand, A. J. Direct Access to the Cooperative Substructure of Proteins and the Protein Ensemble via Cold Denaturation. *Nat. Struct. Mol. Biol.* **2004**, *11*, 352–357.

(15) Jonas, J.; Ballard, L.; Nash, D. High-Resolution, High-Pressure NMR Studies of Proteins. *Biophys. J.* **1998**, *75*, 445 – 452.

(16) Patel, B. A.; Debenedetti, P. G.; Stillinger, F. H.; Rossky, P. J. A Water-Explicit Lattice Model of Heat-, Cold-, and Pressure-Induced Protein Unfolding. *Biophys. J.* **2007**, *93*, 4116 – 4127.

(17) Patel, B. A.; Debenedetti, P. G.; Stillinger, F. H.; Rossky, P. J. The Effect of Sequence on the Conformational Stability of a Model Heteropolymer in Explicit Water. *J. Chem. Phys.* **2008**, *128*, 175102.

(18) Dias, C. L.; Ala-Nissila, T.; Karttunen, M.; Vattulainen, I.; Grant, M. Microscopic Mechanism for Cold Denaturation. *Phys. Rev. Lett.* **2008**, *100*, 118101.

(19) Strambini, G.; Gabellieri, E. Proteins in Frozen Solutions: Evidence of Ice-Induced Partial Unfolding. *Biophys. J.* **1996**, *70*, 971–976.

(20) Chang, B. S.; Kendrick, B. S.; Carpenter, J. F. Surface-Induced Denaturation of Proteins during Freezing and its Inhibition by Surfactants. *J. Pharm. Sci.* **1996**, *85*, 1325 – 1330.

(21) Schwegman, J. J.; Carpenter, J. F.; Nail, S. L. Evidence of partial unfolding of proteins at the ice/freeze-concentrate interface by infrared microscopy. *J. Pharm. Sci.* **2009**, *98*, 3239 – 3246.

(22) Strambini, G. B.; Gonnelli, M. Protein Stability in Ice. *Biophys. J.* **2007**, *92*, 2131–2138.

(23) Eckhardt, B. M.; Oeswein, J. Q.; Bewley, T. A. Effect of freezing on aggregation of human growth hormone. *Pharm. Res.* **1991**, *8*, 1360–1364.

(24) Bhatnagar, B. S.; Pikal, M. J.; Bogner, R. H. Study of the Individual Contributions of Ice Formation and Freeze-Concentration on Isothermal Stability of Lactate Dehydrogenase during Freezing. *J. Pharm. Sci.* **2008**, *97*, 798 – 814.

(25) Timasheff, S. N. The Control of Protein Stability and Association by Weak Interactions with Water: How Do Solvents Affect These Processes? *Annu. Rev. Biophys. Biomol. Struct.* **1993**, *22*, 67–97.

(26) Laio, A.; Parrinello, M. Escaping Free-Energy Minima. *Proc. Natl. Acad. Sci.* **2002**, *99*, 12562–12566.

(27) Pfaendtner, J.; Bonomi, M. Efficient Sampling of High-Dimensional Free-Energy Landscapes with Parallel Bias Metadynamics. *J. Chem. Theory Comput.* **2015**, *11*, 5062–5067.

(28) Wang, Y.; Valsson, O.; Tiwary, P.; Parrinello, M.; Lindorff-Larsen, K. Frequency Adaptive Metadynamics for the Calculation of Rare-Event Kinetics. *J. Chem. Phys.* **2018**, *149*, 072309.

(29) Scalley, M. L.; Yi, Q.; Gu, H.; McCormack, A.; Yates, J. R.; Baker, D. Kinetics of Folding of the IgG Binding Domain of Peptostreptoccocal Protein L. *Biochemistry* **1997**, *36*, 3373–3382.

(30) Scalley, M. L.; Baker, D. Protein Folding Kinetics Exhibit an Arrhenius Temperature Dependence when Corrected for the Temperature Dependence of Protein Stability. *Proc. Natl. Acad. Sci. USA* **1997**, *94*, 10636–10640.

(31) Plaxco, K. W.; Baker, D. Limited Internal Friction in the Rate-Limiting Step of a Two-State Protein Folding Reaction. *Proc. Natl. Acad. Sci. USA* **1998**, *95*, 13591–13596.

(32) Cellmer, T.; Douma, R.; Huebner, A.; Prausnitz, J.; Blanch, H. Kinetic Studies of Protein L Aggregation and Disaggregation. *Biophys. Chem.* **2007**, *125*, 350 – 359.

(33) Kim, D. E.; Fisher, C.; Baker, D. A Breakdown of Symmetry in the Folding Transition State of Protein L. *J. Mol. Biol.* **2000**, *298*, 971 – 984.

(34) Yi, Q.; Scalley, M. L.; Simons, K. T.; Gladwin, S. T.; Baker, D. Characterization of the Free Energy Spectrum of Peptostreptococcal Protein L. *Fold Des.* **1997**, *2*, 271 – 280.

(35) Karanicolas, J.; Brooks, C. L. The Origins of Asymmetry in the Folding Transition States of Protein L and Protein G. *Protein Sci.* **2002**, *11*, 2351–2361.

(36) Yap, E.-H.; Fawzi, N. L.; Head-Gordon, T. A Coarse-Grained α-Carbon Protein Model with Anisotropic Hydrogen-Bonding. *Proteins* **2008**, *70*, 626–638.

(37) Abraham, M. J.; Murtola, T.; Schulz, R.; Pall, S.; Smith, J. C.; Hess, B.; Lindahl, E. GROMACS: High Performance Molecular Simulations through Multi-Level Parallelism from Laptops to Supercomputers. *SoftwareX* **2015**, *1-2*, 19 – 25.

(38) Tribello, G. A.; Bonomi, M.; Branduardi, D.; Camilloni, C.; Bussi, G. PLUMED 2: New Feathers for an Old Bird. *Comput. Phys. Commun.* **2014**, *185*, 604 – 613.

(39) Wikstroem, M.; Drakenberg, T.; Forsen, S.; Sjoebring, U.; Bjoerck, L. Three-Dimensional Solution Structure of an Immunoglobulin Light Chain-Binding Domain of Protein L. Comparison with the IgG-Binding Domains of Protein G. *Biochemistry* **1994**, *33*, 14011–14017, PMID: 7947810.

(40) Jorgensen, W. L.; Maxwell, D. S.; Tirado-Rives, J. Development and Testing of the OPLS All-Atom Force Field on Conformational Energetics and Properties of Organic Liquids. *J. Am. Chem. Soc.* **1996**, *118*, 11225–11236.

(41) Jorgensen, W. L.; Chandrasekhar, J.; Madura, J. D.; Impey, R. W.; Klein, M. L. Comparison of Simple Potential Functions for Simulating Liquid Water. *J. Chem. Phys.* **1983**, *79*, 926–935.

(42) Kony, D.; Damm, W.; Stoll, S.; Van Gunsteren, W. F. An Improved OPLS-AA Force Field for Carbohydrates. *J. Comput. Chem.* **2002**, *23*, 1416–1429.

(43) Masakazu, M.; Takuma, Y.; Hideki, T. GenIce: Hydrogen-Disordered Ice Generator. *J. Comput. Chem.* **2018**, *39*, 61–64.

(44) Essmann, U.; Perera, L.; Berkowitz, M. L.; Darden, T.; Lee, H.; Pedersen, L. G. A Smooth Particle Mesh Ewald Method. *J. Chem. Phys.* **1995**, *103*, 8577–8593.

(45) Berendsen, H. J. C.; Postma, J. P. M.; van Gunsteren, W. F.; DiNola, A.; Haak, J. R. Molecular Dynamics with Coupling to an External Bath. *J. Chem. Phys.* **1984**, *81*, 3684–3690.

(46) Bussi, G.; Donadio, D.; Parrinello, M. Canonical Sampling through Velocity Rescaling. *J. Chem. Phys.* **2007**, *126*, 014101.

(47) Parrinello, M.; Rahman, A. Polymorphic Transitions in Single Crystals: A New Molecular Dynamics Method. *J. Appl. Phys.* **1981**, *52*, 7182–7190.

(48) Tiwary, P.; Parrinello, M. A Time-Independent Free Energy Estimator for Metadynamics. *J. Phys. Chem. B* **2015**, *119*, 736–742.

(49) Russell, R. B.; Barton, G. J. Multiple Protein Sequence Alignment from Tertiary Structure Comparison: Assignment of Global and Residue Confidence Levels. *Proteins* **1992**, *14*, 309–323.

(50) Arsiccio, A.; McCarty, J.; Pisano, R.; Shea, J.-E. Effect of surfactants on surface-induced denaturation of proteins: Evidence of an orientation-dependent mechanism. *J. Phys. Chem. B* **2018**, *122*, 11390–11399.

(51) Kuntz, I. D.; Brassfield, T. S.; Law, G. D.; Purcell, G. V. Hydration of Macromolecules. *Science* **1969**, *163*, 1329 – 1331.

(52) Usha, M. G.; Wittebort, R. J. Orientational Ordering and Dynamics of the Hydrate and Exchangeable Hydrogen Atoms in Crystalline Crambin. *J. Mol. Biol.* **1989**, *208*, 669 – 678.

(53) Siemer, A. B.; Huang, K.-Y.; McDermott, A. E. Protein–Ice Interaction of an Antifreeze Protein Observed with Solid-State NMR. *Proc. Natl. Acad. Sci. USA* **2010**, *107*, 17580–17585.

(54) Tompa, K.; Bánki, P.; Bokor, M.; Kamasa, P.; Lasanda, G.; Tompa, P. Interfacial Water at Protein Surfaces: Wide-Line NMR and DSC Characterization of Hydration in Ubiquitin Solutions. *Biophys. J.* **2009**, *96*, 2789 – 2798.

(55) Bhatnagar, B.; Zakharov, B. A.; Fisyuk, A. S.; Wen, X.; Karim, F. Z.; Lee, K.; Seryotkin, Y. V.; Mogodi, M.; Fitch, A.; Boldyreva, E.; Kostyuchenko, A.; Shalaev, E. Protein/ice Interaction: High-Resolution Synchrotron X-Ray Diffraction Differentiates Pharmaceutical Proteins From Lysozyme. *J. Phys. Chem. B* **2019**, *123*, 5690–5699.

(56) Knight, C. A.; DeVries, A. L. Ice Growth in Supercooled Solutions of a Biological "Antifreeze", AFGP 1–5: An Explanation in Terms of Adsorption Rate for the Concentration Dependence of the Freezing Point. *Phys. Chem. Chem. Phys.* **2009**, *11*, 5749–5761.

(57) Marks, S. M.; Patel, A. J. Antifreeze Protein Hydration Waters: Unstructured Unless Bound to Ice. *Proc. Natl. Acad. Sci.* **2018**, *115*, 8244–8246.

(58) Chau, P.-L.; Hardwick, A. J. A New Order Parameter for Tetrahedral Configurations. *Mol. Phys.* **1998**, *93*, 511–518.

(59) van der Spoel, D.; van Maaren, P. J.; Larsson, P.; Timneanu, N. Thermodynamics of Hydrogen Bonding in Hydrophilic and Hydrophobic Media. *J. Phys. Chem. B* **2006**, *110*, 4393–4398.

(60) Luzar, A.; Chandler, D. Hydrogen-Bond Kinetics in Liquid Water. *Nature* **1996**, *379*, 55–57.

(61) Luzar, A. Resolving the Hydrogen Bond Dynamics Conundrum. *J. Chem. Phys.* **2000**, *113*, 10663–10675.

(62) Arakawa, T.; Kita, Y.; Carpenter, J. F. Protein-Solvent Interactions in Pharmaceutical Formulations. *Pharm. Res.* **1991**, *8*, 285–291.

(63) Arakawa, T.; Timasheff, S. N. Stabilization of Protein Structure by Sugars. *Biochemistry* **1982**, *21*, 6536–6544.

(64) Arsiccio, A.; Pisano, R. Clarifying the Role of Cryo- and Lyo-Protectants in the Biopreservation of Proteins. *Phys. Chem. Chem. Phys.* **2018**, *20*, 8267–8277.

Graphical TOC Entry